

## **New Modeling of Metal Oxide Surge Arresters**

**Seyed Mohammad Hassan Hosseini<sup>1\*</sup>, Younes Gharadaghi<sup>1</sup>**

<sup>1</sup> Electrical Engineering Department, South Tehran Branch, Islamic Azad University, Tehran, Iran.

### **Abstract**

This paper describes simplified modeling of metal oxide surge arrester (MOSA) to operate analysis. This model is a new model proposed (P-K Model) to verify the accuracy in order to compare with IEEE and Pinceti Model. The simulations are performed with the Alternative Transients Program version of Electromagnetic Transient Program (ATP-EMTP). In the present paper, the MOSA models were verified for several medium voltages which consist of 18 kV and 21 kV, which 18 kV arrester was used in 22 kV system of Provincial Electricity Authority (PEA) and 21 kV arrester was used in 24 kV system of Metropolitan Electricity Authority (MEA) in Thailand. The P-K model was evaluate from different manufacturing, it is based on the General Electric (GE), Siemens and Ohio Brass as well as IEEE and Pinceti Model. The tests are performed by applying a fast front current surge with front time of up to  $0.5\mu\text{s}$  and the standard impulse current surge ( $8/20\mu\text{s}$ ). The results were compared between three models in order to calculate the error operation of the MOSA in the ATP-EMTP Program. The relative error of arrester models show that the P-K model can be used to simulate and calculate in ATP-EMTP program as well as IEEE and Pinceti model. In the case of fast front current surge, the P-K model has a maximum error of 5.39% (Ohio Brass, 10 kA, 21 kV) and has a minimum error of 0.24% (GE, 10 kA, 18 kV). Also, the standard impulse current surge, P-K model has a maximum error of 2% (Ohio Brass, 10 kA, 18 kV) and has a minimum error of 0.32% (Siemens, 10 kA, 21 kV) in the voltage response.

**Keywords:** Oxide Surge Arrester, Frequency-Dependent Model, Lightning and Overvoltage.

---

### **1. INTRODUCTION**

The metal oxide varistor (MOV) material [1] used in modern high voltage surge arresters has a highly non-linear voltage versus current characteristic. The V-I

characteristic is dependent upon wave shape of the arrester current. The physical construction of modern high voltage surge arresters consists of metal Oxide discs in-

---

\*Corresponding Author's Email: smhh110@azad.ac.ir

side a porcelain or polymer insulator.

A higher voltage is achieved by adding disks in series. Higher energy ratings are achieved by using larger diameter discs or parallel columns of discs. The highly non-linear V-I characteristic obviates the need for series spark gaps. The electrical characteristics are determined solely by the properties of the metal oxide blocks.

The ATP-EMTP, Alternative Transients Program version of Electromagnetic Transient Program [2], program allows the modeling of this non-linear resistance through the ZnO Fitter routine and the Type 92. Laboratory test data of metal oxide arrester discharge voltage and current have indicated that the arrester has dynamic characteristics that are significant for studies involving fast front surges, which are not well represented by the ATP model previously mentioned. Technical data show that for fast front surges, with rise time less than  $8\mu\text{s}$ , the voltage waveform peak occurs before the current waveform peak and the residual voltage across the arrester increases as the time to crest of the arrester discharge current decreases.

The increase could reach approximately 6% when the front time of the discharge is reduced from  $8\mu\text{s}$  to  $1.3\mu\text{s}$ .

According to [3], this peak can reach up to 12%. It may be pointed out that the voltage across the arrester is not only a function of the magnitude of the discharge current, but it is also dependent on the rate of increase. This fact is particularly important in lightning studies. Several models, at different voltage levels, have been proposed to represent the frequency dependent characteristic of metal oxide surge arresters. The model proposed by the IEEE Working Group, although having the purpose of finding a mathematical model that ade-

quately reproduces these effects without requiring excessive computing time, uses a trial and error procedure.

The purpose of this paper is to present a simplified model for metal oxide surge arrester (MOSA), and was conducted to a comparison of several models [3, 4]. These models have been proposed to simulate these dynamic characteristics. The results show that all models have similar performance when subjected to fast front surge current and standard impulse current surge.

## 2. THE IEEE MODEL

The IEEE model was recommended by IEEE W.G. 3.4.11 [3], is shown in Fig.1. The  $A_0$  and  $A_1$  are the two non-linear resistances and they are separated by a RL filter. For arrester discharge currents with slow rising time, the influence of the filter is negligible; thus  $A_0$  and  $A_1$  are essentially parallel and characterize the static behavior of the MOSA. For fast front surge currents, the impedance of the filter becomes more significant, indeed the inductance  $L_1$  derives more current into the non-linear branch  $A_0$ . Since  $A_0$  has a higher voltage for a given current than  $A_1$ , the model generates a higher voltage between its input terminals, which matches the dynamic characteristics of MOSAs.

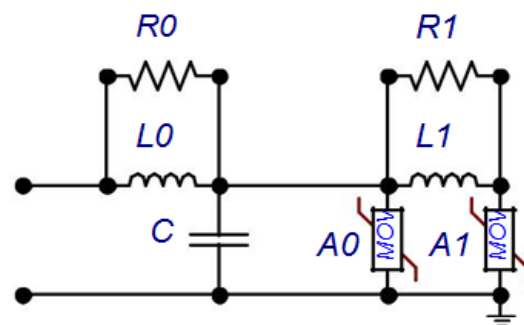


Fig. 1. IEEE Frequency-dependent model.

The proposed curves for  $A_0$  and  $A_1$  are shown in Fig.2 [5]. The per-unit values are referred to the peak value of the residual voltage measured during a discharge test with 10 kA standard impulse current surge ( $V_{r,8/20}$ ). These curves are to be adjusting to get a good fit with the published residual voltages for switching surge discharge currents. The inductance  $L_0$  represents the inductance associated with the magnetic fields in the immediate vicinity of the arrester.

The resistor  $R_0$  is used to avoid numerical oscillations when running the model with a digital program. The capacitance  $C_0$  represents the external capacitance associated to the height of the arrester. Starting from the physical dimensions of the arrester, some formulas are given in [1] to calculate  $L_0$ ,  $R_0$ ,  $C_0$  and  $R_1$ .

The parameter  $L_1$  has the most influence on the result and a formula, starting from the physical dimensions, is also suggests in [1]. However this constitutes only an initial value and  $L_1$  should be adjusted by a try- and error procedure to match the residual voltages for lightning discharge currents published in manufacture's catalogue. This model can give satisfactory results for discharge currents within a range of times to crest for 0.5  $\mu$ s to 45  $\mu$ s.

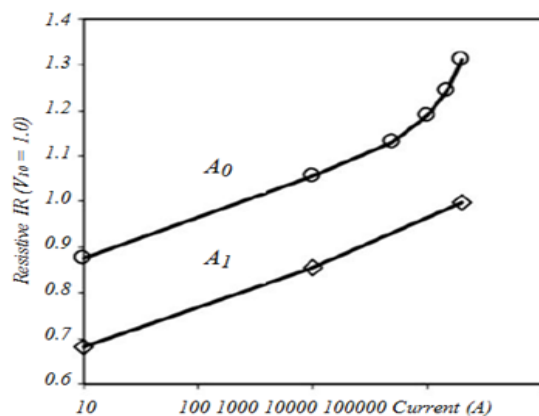


Fig. 2. Non-linear characteristic for  $A_0$  and  $A_1$ .

### 3. THE PINCETI MODEL

The PINCETI model [4] presents derives from the IEEE model, with some minor differences. By comparing the models in Fig.1 and Fig.3, it can be noted that:

The capacitance is eliminated, since its effects on model behavior is negligible, the two resistances in parallel with the inductances are replaced by one resistance  $R$  (about 1 M $\Omega$ ) between the input terminals, with the only a scope to avoid numerical troubles.

The operating principle is quite similar to that of the IEEE frequency-dependent model. The parameter definition will be shown that the proposed model can be easily defined by adopting the two following rules:

The definition of non-linear resistors characteristics ( $A_0$  and  $A_1$ ) is based on the curves shown in Fig. 2. These curves derives from the curves proposed by IEEE W.G. 3.4.11, and are referred to the peak value of the residual voltage measured during a discharge test with a 10 kA lightning current impulse ( $V_{r,8/20}$ ); - to define the inductances, the following equations can be used (values are in  $\mu$ H):

$$L_1 \frac{1}{4} \cdot \frac{V_{r1} V_{r8/20}}{V_{r8/20}} \cdot V_N \quad (1)$$

$$L_0 \frac{1}{12} \cdot \frac{V_{r1} V_{r8/20}}{V_{r8/20}} \cdot V_N \quad (2)$$

where:

$V_N$  = is the arrester rated voltage

$V_{r1/T2}$  = residual voltage at 10 kA fast front current surge ( $1/T_2 \mu$ s). The decrease time is not explicitly written because different manufacturers may use different values. This fact does not cause any trouble, since the peak

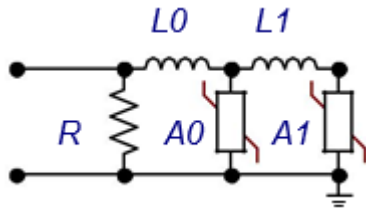


Fig. 3. PINCETI model.

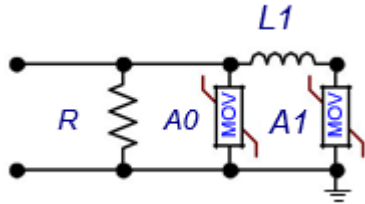


Fig. 4. P-K model

value of the residual voltage appears on the rising front of the impulse.

$V_{r8/20}$  = residual voltage at 10 kA current surge with a 8/20  $\mu$ s shape.

The proposed criteria do not take into consideration any physical characteristic of the arrester. Only electrical data are needed. The equations (1) and (2) are based on the fact that parameters  $L_0$  and  $L_1$  are related to the roles that these elements have in the model. In other words, since the function of the inductive elements is to characterize the model behavior with respect to fast surges, it seemed logical to define these elements by means of data related to arrester behavior during fast surges.

#### 4. THE PROPOSED MODEL (P-K MODEL)

The proposed model (P-K model) is shown in Fig. 4 and derives from P-K model that in [4]. It is intended for the simulation of the dynamic characteristics for discharge currents with front times starting from 0.5 to 8  $\mu$ s. As in [4], between the non-linear resistances  $A_0$  and  $A_1$  only the inductance  $L_1$ , which is defined the inductance, the following equations can be used (values are in  $\mu$ H):

$$L_1 = \frac{9}{10} \cdot \frac{V_{r1} V_{r8}}{V_{r8/20}} \cdot V_n \quad (3)$$

The resistance (R) has about 1 M to install between the input terminals.

#### 5. SIMULATION RESULTS

The simulations were performed with ATP-EMTP program. The fast front current surge and the standard impulse current surge of each model for the 0.5 $\mu$ s and 8/20 $\mu$ s were presented at 18 kV and 21 kV in Table 2 and 3 respectively. In these tables, the relative error ( $H_r$ ) in % defined by (4). Technical data of several arresters are reported in Table 1.

$$H_r = \frac{V_{rsim} V_{rman}}{V_{rman}} \cdot 100 \quad (4)$$

where:

Table 1. Technical data of the considered arrester.

Manuf.	Rate	0.5 $\mu$ sec	8/20 $\mu$ s Maximum Discharge			
	Voltage	10 kA	Voltage			
GE	(kV)	IR-kVcrest	3 kA	5 kA	10 kA	20 kA
	18	65	49	52	57.5	65.4
	21	69.5	52.5	55.7	61.5	69.9
Siemens	18	52.5	42.5	44.4	47.7	53.4
	21	56.9	47.7	49.9	53.8	59.6
Ohio Brass	18	51.6	43.2	45.2	48.8	54
	21	61.2	49.5	51.8	55.7	62.3

**Table 2. Calculation residual voltage and relative error (18 kV arrester).**

Model	Manuf.	Index	8/20 $\mu$ s Maximum Discharge Voltage				
			0.5 $\mu$ sec 10 kA IR-kV <sub>crest</sub>	3 kA	5 kA	10 kA	20 kA
IEEE	GE	V <sub>r</sub>	65.45	64	54.40	57.46	62.35
		H <sub>r</sub>	0.69	7.43	!	-0.06	-4.66
	Siemens	V <sub>r</sub>	54.81	43.67	45.14	47.69	51.83
		H <sub>r</sub>	4.41	2.75	1.66	-0.002	-2.94
	Ohio Brass	V <sub>r</sub>	55.75	44.68	46.18	48.78	52.96
		H <sub>r</sub>	8.03	3.42	2.17	-0.02	-1.91
PINCE	GE	V <sub>r</sub>	64.26	52.44	53.74	55.96	59.3
		H <sub>r</sub>	-1.13	7.02	3.35	-2.67	-9.32
	Siemens	V <sub>r</sub>	52.77	43.5	44.55	46.36	49.02
		H <sub>r</sub>	0.53	2.35	0.35	2.79	-8.2
	Ohio Brass	V <sub>r</sub>	50.94	44.48	45.49	47.23	49.41
		H <sub>r</sub>	-1.27	2.98	0.65	-3.2	-8.48
P-K	GE	V <sub>r</sub>	65.15	52.72	54.62	58	63.13
		H <sub>r</sub>	0.24	7.6	5.08	0.87	-3.47
	Siemens	V <sub>r</sub>	54	43.7	45.22	47.9	52.09
		H <sub>r</sub>	2.95	2.82	1.85	0.43	-2.45
	Ohio Brass	V <sub>r</sub>	54.23	44.54	45.76	47.82	51.13
		H <sub>r</sub>	5.09	3.1	1.247	-2	-5.3

**Table 3. Calculation residual voltage and relative error (21 kV arrester).**

Model	Manuf.	Index	8/20 $\mu$ s Maximum Discharge Voltage				
			5 $\mu$ sec 10 kA R-kV <sub>crest</sub>	3 kA	5 kA	10 kA	20 kA
IEEE	GE		69.96	56.3	58.21	61.51	66.76
			0.67	7.26	4.5	0.01	-4.49
	Siemens		64.22	51.0	52.75	55.81	60.71
			4.94	3.09	1.85	0.2	-2.55
	Ohio Brass		61.45	49.2	50.91	53.78	58.37
			7.99	3.26	2.02	-0.03	-2.05
PIN CETI	GE		69.3	56.1	57.51	59.93	63.64
			-0.28	6.85	3.26	-2.55	-8.95
	Siemens		61.5	50.7	52.02	54.13	57.2
			0.5	2.62	0.43	-2.81	-8.18
	Ohio Brass		56.41	49.0	50.16	52.08	54.52
			-0.84	2.82	0.52	-3.19	-8.52
P-K	GE		69.81	56.4	58.58	62.4	67.95
			0.45	7.54	5.18	1.46	-2.78
	Siemens		63.02	51.0	52.78	55.88	60.74
			2.97	3.07	1.89	0.32	-2.49
	Ohio Brass		59.96	49.1	50.49	52.81	56.59
			5.39	2.96	1.19	-1.83	-5.05

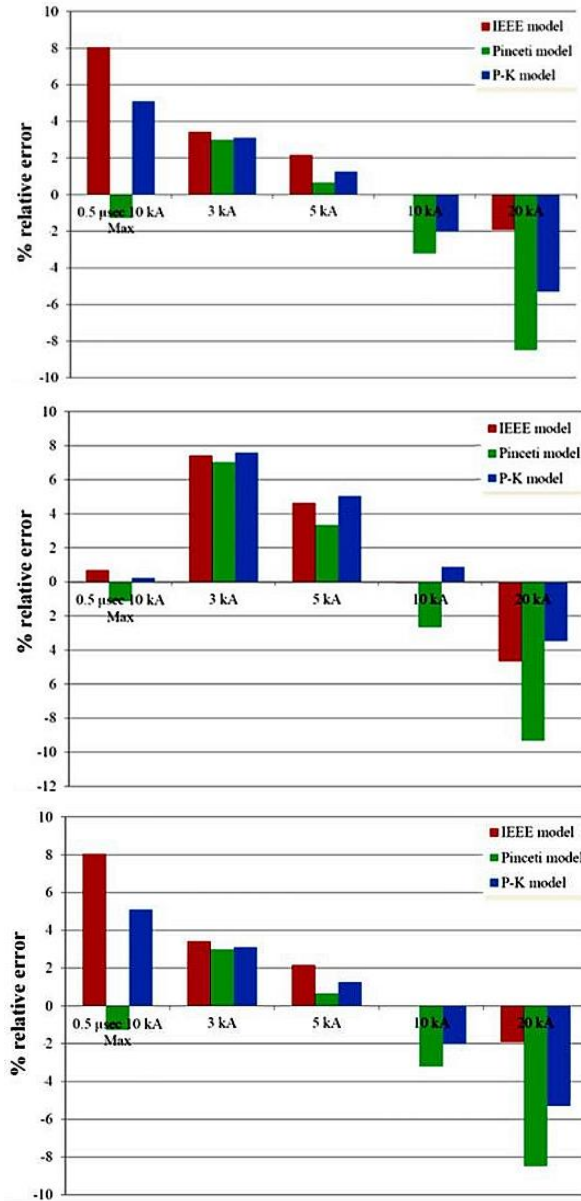


Fig. 5. Relative error on residual voltage, 18 kV (a) GE; (b) Siemens; (c) Ohio Brass.

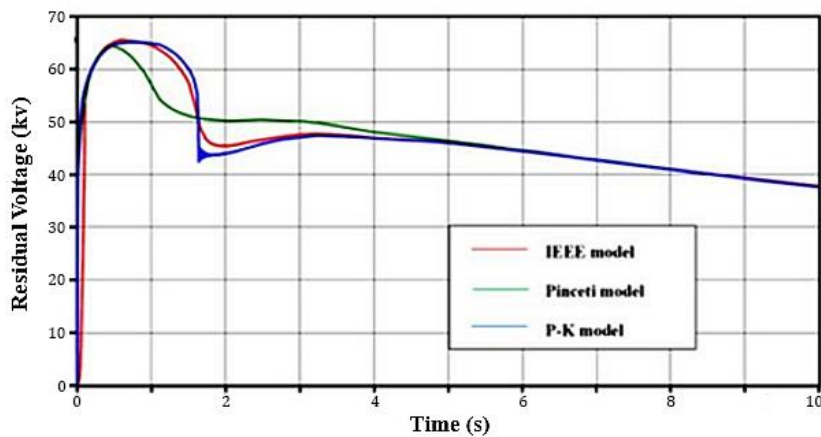
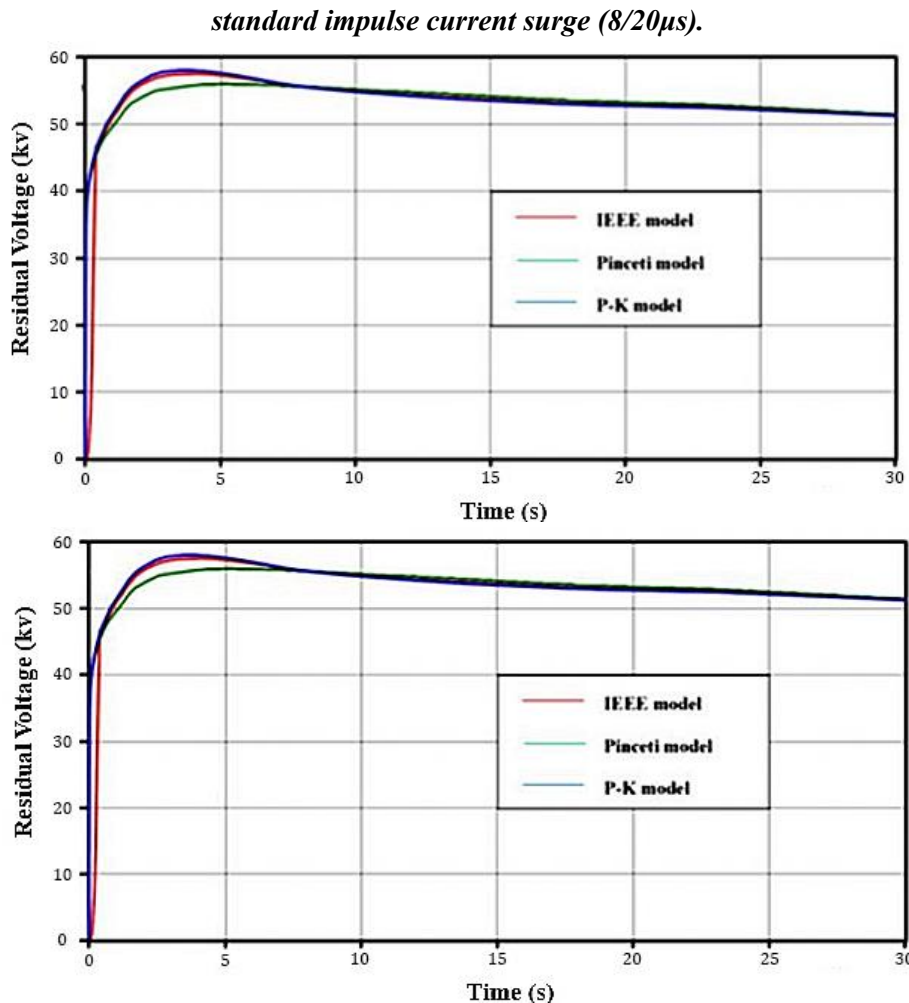


Fig. 6. The arrester product of GE 10 kA, 18 kV (a) The fast front current surge (0.5μs); (b) The



**Fig. 7. The arrester product of Siemens 10 kA, 18 kV (a) The fast front current surge (0.5 $\mu$ s); (b) The standard impulse current surge (8/20 $\mu$ s).**

$V_{rsim}$  : is the simulated residual voltage;  
 $V_{rman}$  : is the manufacturer's residual voltage

The relative error on residual voltage with each manufacturer which consists of GE, Siemens and Ohio Brass at 18 kV is shown in Fig. 5.

The residual voltage results of the fast front current surge (0.5 $\mu$ s) and the standard impulse current surge (8/20 $\mu$ s) for current amplitude of 10 kA at 18 kV are presented in Figs. 6, 7 and 8.

The relative error on residual voltage with each manufacturer which consists of GE, Siemens and Ohio Brass at 21 kV is shown in

Fig. 9.

The residual voltage results of the fast front current surge (0.5 $\mu$ s) and the standard impulse current surge (8/20 $\mu$ s) for current amplitude of 10 kA at 21 kV are presented in Figs. 10, 11 and 12.

## 6. CONCLUSION

In this paper, the dynamic behavior of metal oxide surge arrester models is simulated with fast front time of up to 0.5 $\mu$ s and standard impulse current surge (8/20 $\mu$ s) which consist of IEEE, Pinceti and P-K model. The

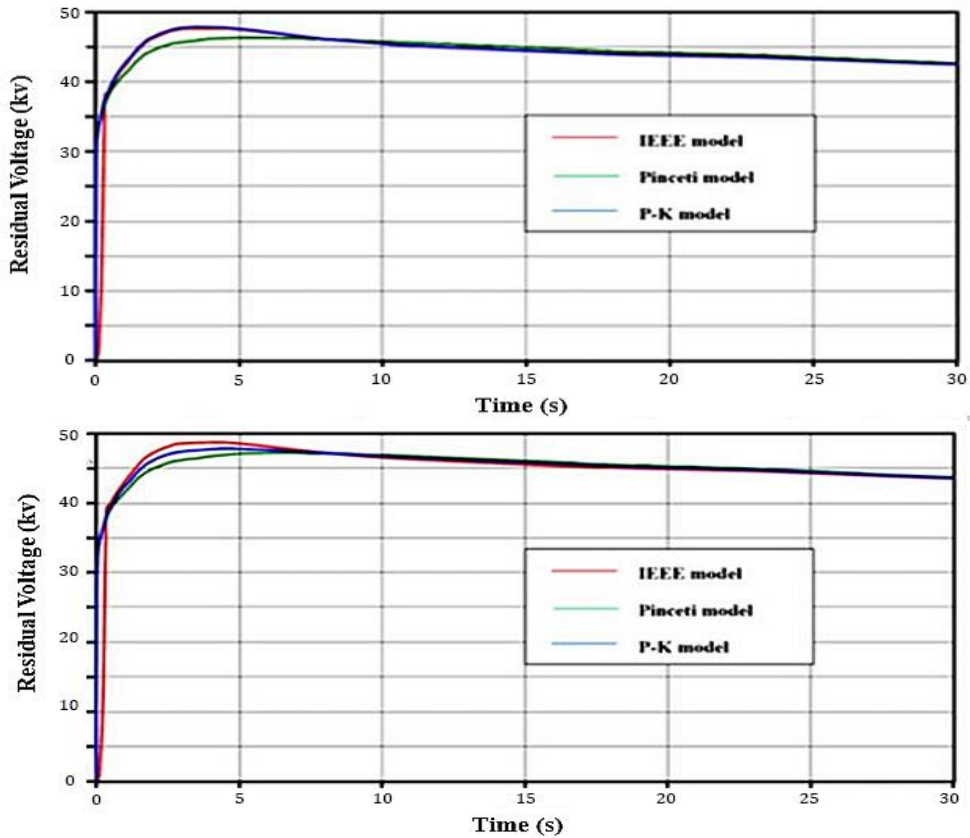


Fig. 8. The arrester product of Ohio Brass 10 kA, 18 kV (a) The fast front current surge (0.5 $\mu$ s); (b) The standard impulse current surge (8/20 $\mu$ s).

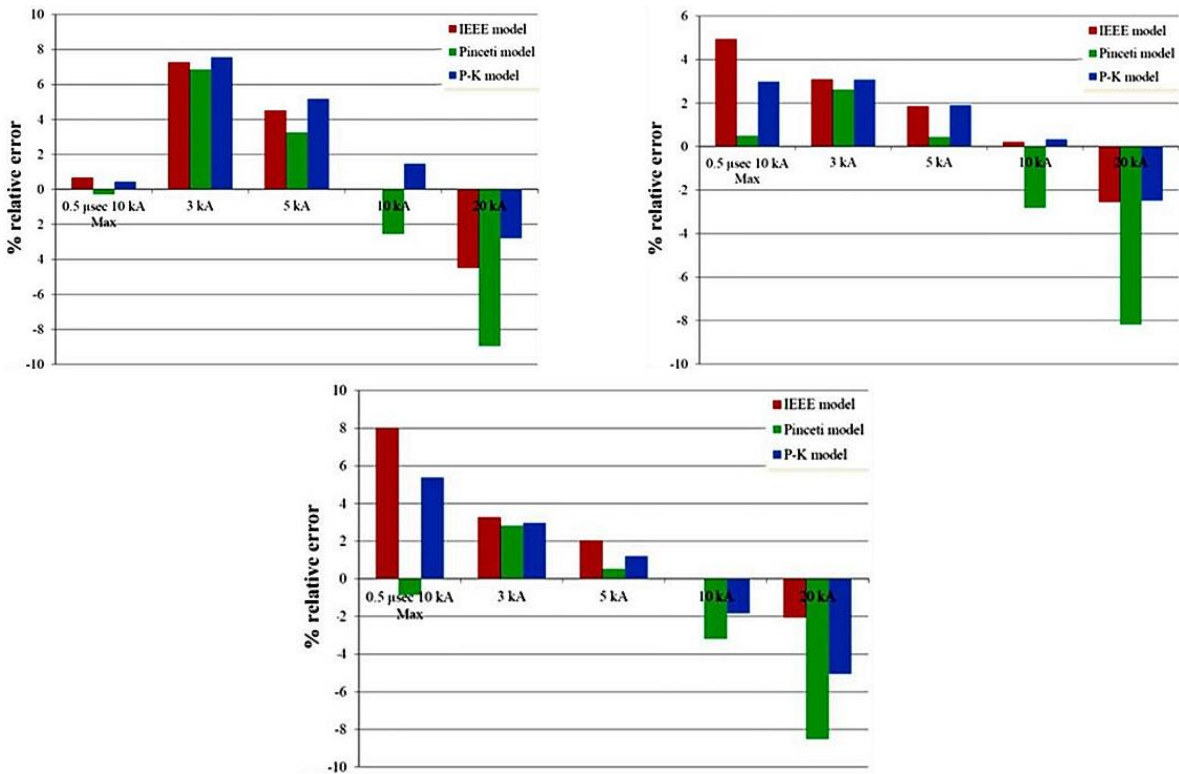


Fig. 9. Relative error on residual voltage, 21 kV (a) GE; (b) Siemens; (c) Ohio Brass.

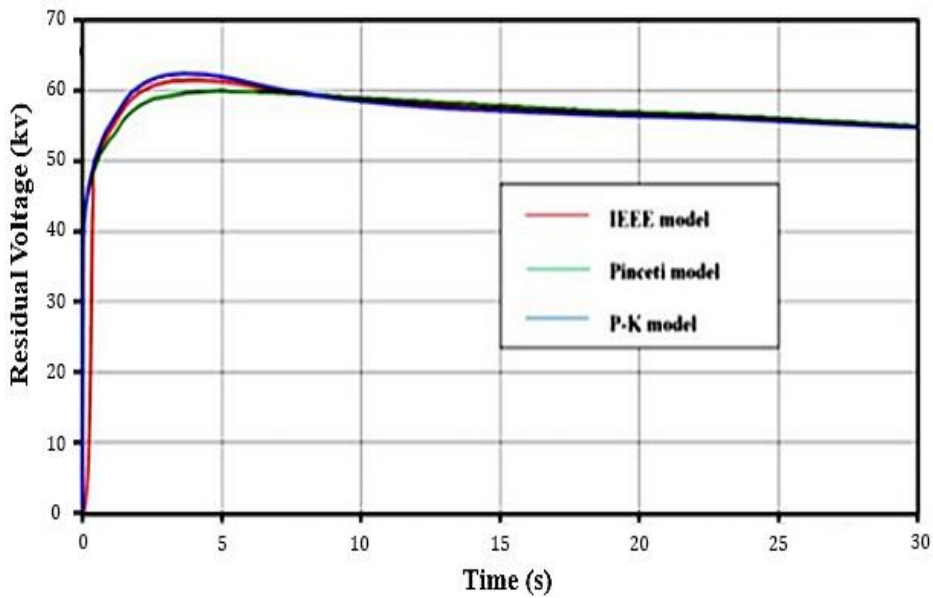
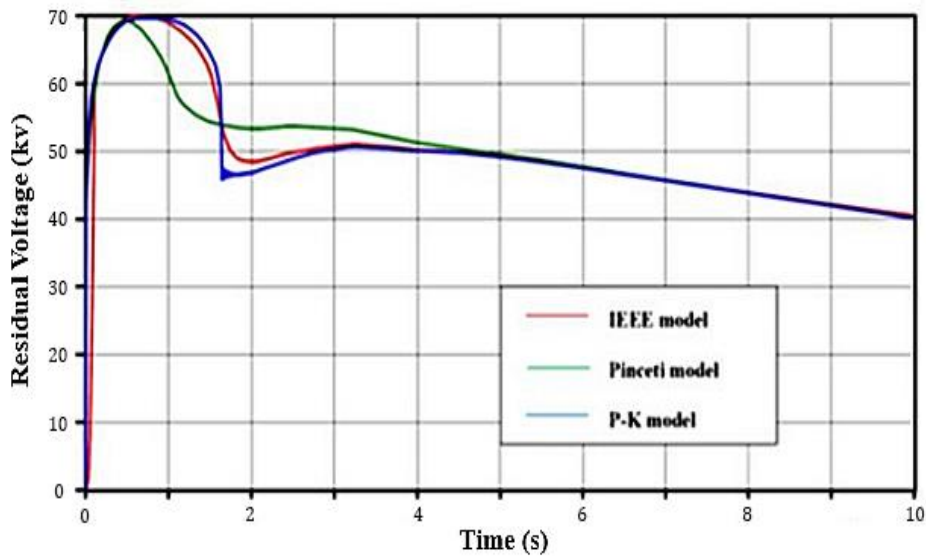
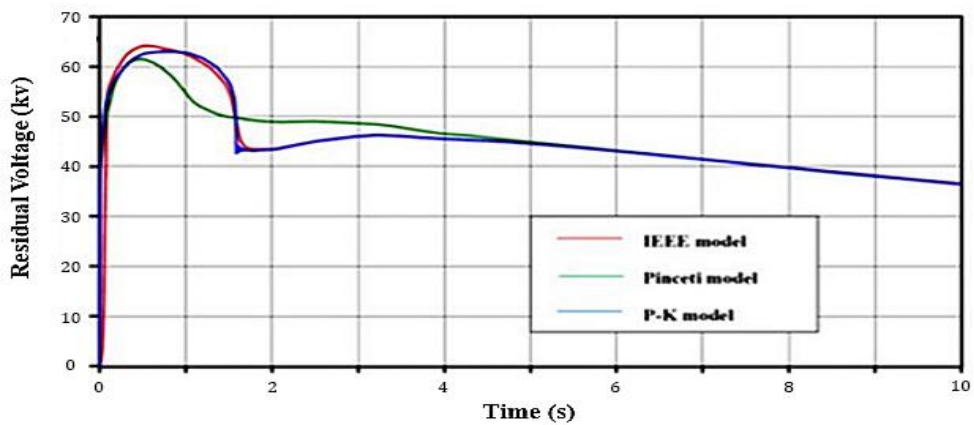
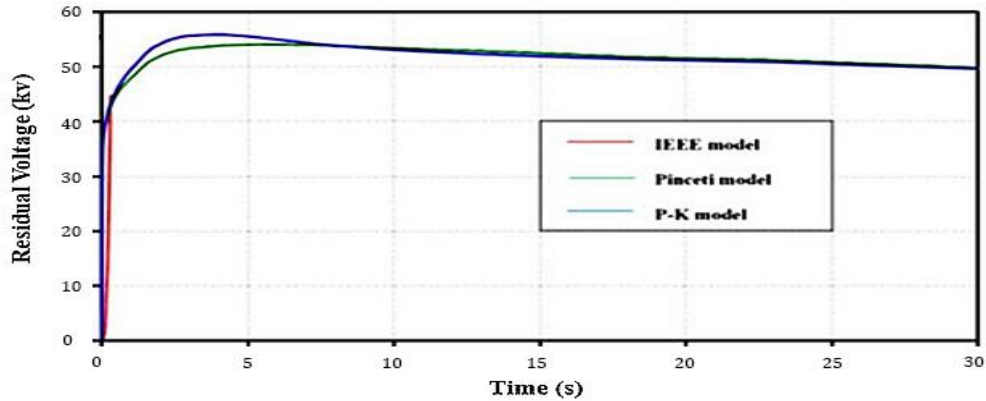
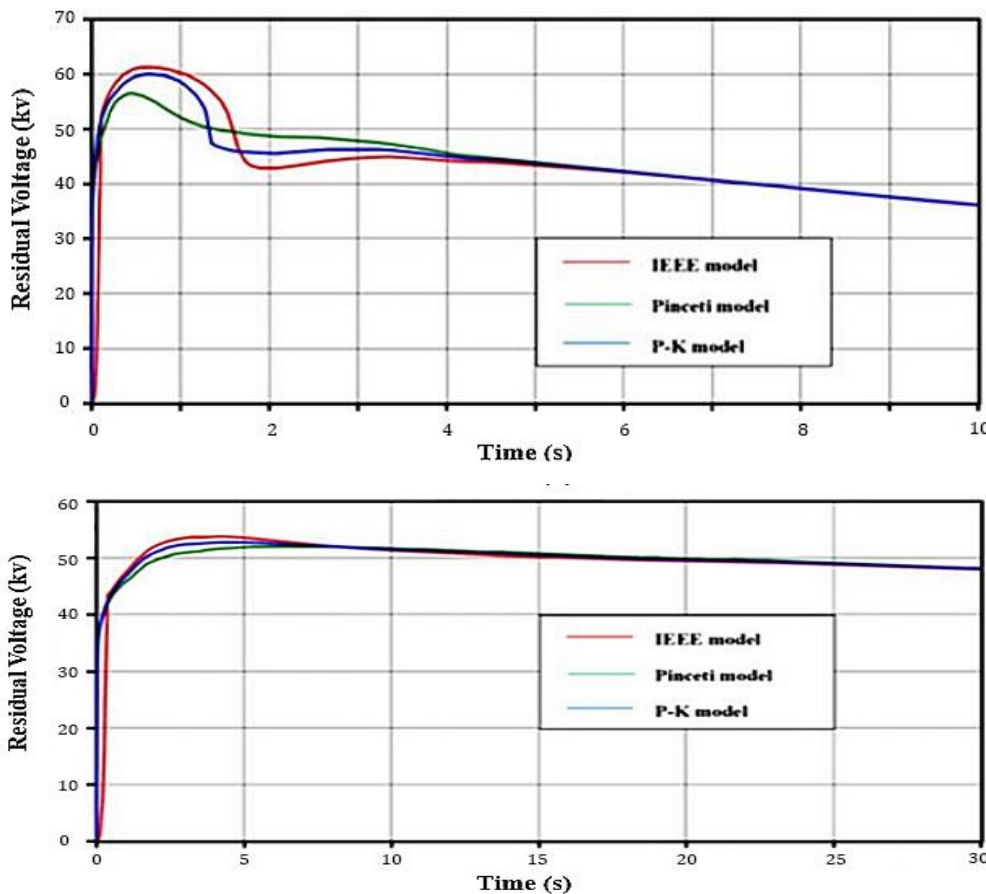


Fig. 10. The arrester product of GE 10 kA, 21 kV (a) The fast front current surge (0.5µs); (b) The standard impulse current surge (8/20µs).





**Fig. 11.** The arrester product of Siemens 10 kA, 21 kV (a) The fast front current surge ( $0.5\mu\text{s}$ ); (b) The standard impulse current surge ( $8/20\mu\text{s}$ ).



**Fig. 12.** The arrester product of Ohio Brass 10 kA, 21 kV (a) The fast front current surge ( $0.5\mu\text{s}$ ); (b) The standard impulse current surge ( $8/20\mu\text{s}$ ).

simulations of MOSA models were performed with the ATP-EMTP program. These three modeling results were compared with the data reported on the several manufacturer's catalogue, it was given to demonstrate the accuracy of models. The simulations of

P-K model have been shown that it can use acceptably with a fast front current surge and standard impulse current surge at 18 kV and 21 kV in PEA and MEA respectively. In the case of fast front current surge, the IEEE model has a maximum error of 8.03% (10

kA, 18 kV), the Pinceti model has a maximum error of 1.27% (10 kA, 18 kV), and P-K model has a maximum error of 5.39% (10 kA, 21 kV). And also, the standard impulse current surge, the IEEE model has a maximum error of 7.43% (3 kA, 18 kV), the Pinceti model has a maximum error of 9.32% (20 kA, 18 kV), and P-K model has a maximum error of 7.6% (3 kA, 18 kV) in the voltage response. However, the P-K model can be used to simulate and calculate in ATP-EMTP program as well as IEEE and Pinceti model.

## REFERENCES

- [1] Richard G. Baraniuk , "Compressive Sensing" , IEEE Signal Processing Magazine ,VOL.24 , Issue: 4 , July 2007.
- [2] Jia Li, Zhaojun Wu, Hongqi Feng, Qiang Wang, "Greedy Orthogonal Matching Pursuit Algorithm for Sparse Signal Recovery in Compressive Sensing", IEEE Region 10 Conference, pp. 1-4, 2015.
- [3] Emmanuel J. Candès and Michael B. Wakin, "An Introduction To Compressive Sampling", IEEE Signal Processing Magazine, Volume: 25, Issue: 2, March 2008.
- [4] Ying Liu and Dimitris A. Pados, "Compressed-Sensed-Domain L1-PCA Video Surveillance", IEEE Transactions on Multimedia, VOL. 18, NO. 3, March 2016.
- [5] Rui Wang, Jinglei Zhang, Suli Ren, and Qingjuan Li, "A Reducing Iteration Orthogonal Matching Pursuit Algorithm for Compressive Sensing" , Tsinghua Science and Technology , pp. 71-79, Vol 21, Number 1, February 2016.
- [6] Donoho, D. , 2006. "Compressed sensing" , IEEE Transaction on Information Theory, Vol. 52, No. 4, pp. 1289-1306.
- [7] Thein Thanh Lam, "Optimization in L1- Norm for sparse recovery", Faculty of Mathematics and Natural Sciences University of Oslo, 2014.